J. Biochem. 2010;148(4):467–479 doi:10.1093/jb/mvq080

JB THE JOURNAL OF BIOCHEMISTRY

Mechanisms and specificity of factor XIa and trypsin inhibition by protease nexin 2 and basic pancreatic trypsin inhibitor

Received June 15, 2010; accepted July 10, 2010; published online July 20, 2010

Duraiswamy Navaneetham[1], Dipali Sinha[1] and Peter N. Walsh[1,2,3,*]

[1]Sol Sherry Thrombosis Research Center; [2]Department of Medicine; and [3]Department of Biochemistry, Temple University School of Medicine, Philadelphia, PA 19140, USA

*Peter N. Walsh, Sol Sherry Thrombosis Research Center, Temple University School of Medicine, 3400 North Broad Street, Philadelphia, PA 19140, USA, Tel:+1 215 707 4375, Fax: +1 215 707 3005, email: pnw@temple.edu

Factor XIa (FXIa) inhibition by protease nexin-2 (PN2KPI) was compared with trypsin inhibition by basic pancreatic trypsin inhibitor (BPTI). PN2KPI was a potent inhibitor of FXIa ($K_i \sim 0.81$ nM) and trypsin ($K_i \sim 0.03$ nM), but not of other coagulation proteases (thrombin, FVIIa, FIXa, FXa, FXIIa, plasmin, kallikrein, $K_i > 185$ nM). PN2KPI was ~775-fold more potent than BPTI in FXIa inhibition, but both exhibited similar potencies against trypsin. Studies of FXIa and trypsin inhibition by PN2KPI and BPTI and P1 site swap mutants (PN2KPI-R15 K, BPTI-K15 R) demonstrated that FXIa inhibition by PN2KPI and P1 site swap mutants and trypsin inhibition by PN2KPI and BPTI conform to a single-step, slow equilibration inhibitory mechanism, whereas FXIa-inhibition by BPTI follows a classical, competitive inhibitory mechanism. Mutation of P1 impaired FXIa inhibition by PN2KPI-R15 K ~14-fold, enhanced FXIa inhibition by BPTI-K15 R ~150-fold, and had no effect on trypsin inhibition. Arginine at the P1 site of either PN2KPI or BPTI confers high affinity and specificity for FXIa, whereas either arginine or lysine suffices for trypsin inhibition. Thus, PN2KPI is a highly specific inhibitor of FXIa among coagulation enzymes, but the flexibility of trypsin renders it susceptible to inhibition by both wild-type and mutant forms of PN2KPI and BPTI.

Keywords: BPTI/FXIa/inhibition mechanism/protease nexin 2 Kunitz domain/trypsin.

Abbreviations: BMMY, buffered medium containing methanol and yeast nitrogen base; BMGY, buffered medium containing glycerol and yeast nitrogen base; BPTI, basic (or bovine) pancreatic trypsin inhibitor; PN2KPI, protease nexin 2 Kunitz protease inhibitory domain; PN2, protease nexin 2; KPI, Kunitz protease inhibitor; FXIIa, factor XIIa; FXIa, factor XIa; FXa, factor Xa; FIXa, factor IXa; FVIIa, factor VIIa; FIIa, factor IIa (thrombin).

Coagulation factor XIa (FXIa), the activated form of the zymogen (FXI), other coagulation enzymes and trypsin are all members of a diverse family of serine peptidases that carry out disparate biological functions (*1*). FXI is a homodimeric 160-kDa glycoprotein, present in human plasma, which is essential for normal haemostasis, since its deficiency is associated with a hemorrhagic disorder termed haemophilia C (*2*). The zymogen is activated by coagulation proteases including thrombin, FXIIa and FXIa (*3–6*). The activation product of this event is FXIa, which in turn can activate FIX to FIXa to initiate the consolidation phase of blood coagulation resulting in fibrin formation at the site of blood vessel injury (*2*, *7–10*). The 30-kDa light-chain region of FXIa is highly homologous to trypsin and harbours its serine protease catalytic activity.

Important control mechanisms exist for the regulation of coagulation protease activities. Serine protease inhibitors (SERPIN) have been proposed as physiological regulators of FXIa function in plasma, including protease nexin 1 (*11*), antithrombin III (*12*), C1 inhibitor (*13*, *14*), α-1-protease inhibitor (*15*, *16*) and α-2-antiplasmin (*17*). On platelet activation by physiological stimulators, protease nexin 2 (PN2) is secreted from α-granules into plasma and inhibits FXIa (*18–20*). PN2, a member of the class of Kunitz-type inhibitors, is a ~120-kDa isoform of the Alzheimer's β-amyloid protein precursor that has been shown to be a highly potent and physiologically relevant inhibitor of FXIa on the basis of detailed kinetic studies (*18*, *19*, *21–24*). PN2 is a slow, tight binding inhibitor of FXIa with a reported K_i of 290–450 pM (*18*, *21*, *23*). The KPI domain of PN2 (PN2KPI) is 57 residues in length (Glu^{289}-Ile^{345} in the 751 amino acid isoform of PN2) and contains the entire FXIa inhibitory function of PN2 (*22–25*). A homologous protein belonging to the same Kunitz family called basic (or bovine) pancreatic trypsin inhibitor (BPTI; aprotinin; Trasylol^{R}) is also an inhibitor of several human serine proteases such as trypsin, plasmin, kallikrein, activated protein C and FXIa (*26*, *27*).

Although a great deal is known about the structural biology of the proteases, FXIa and trypsin, and their inhibitors, PN2KPI and BPTI, very little information is available concerning the mechanisms by which these two Kunitz-type inhibitors regulate the activities of the two serine proteases. The rationale for the present study, which focused on a comparison of the mechanisms of inhibition of human FXIa and bovine trypsin by the human PN2KPI and BPTI, is based on the

striking structural homology between the human FXIa/PN2KPI complex (*28*) and the bovine trypsin/BPTI complex (*29*), in addition to the fact that BPTI (as Trasylol^{R}) is frequently utilized therapeutically in human subjects in the treatment and prevention of thrombo-embolism, *e.g.* in patients undergoing cardiopulmonary bypass surgery (*30*, *31*). Moreover, a large number of naturally occurring nonhuman serine proteinase inhibitors have been identified as potent inhibitors of human proteinases. This category of nonhuman inhibitors includes bovine BPTI (*26*, *27*, *32*, *33*), tick anticoagulant peptide (*34–36*) and Boophilin from the cattle tick (*37*), which inhibit several human enzymes including proteinases in coagulation cascade. Human Kunitz-type inhibitors are also known to inhibit nonhuman proteinases. For example, bovine trypsin and bovine chymotrypsin are inhibited by human TFPI (*38*), TFPI 2 (*39*) and PN2KPI (*21*, *40*), whereas mouse NGF-gamma is inhibited by human PN2KPI (*21*). In addition to these biochemical studies, three-dimensional structures of cross-species enzyme/inhibitor complexes have also been documented, including the crystal structures of human PN2KPI in complex with bovine trypsin, bovine chymotrypsin (*41*), and rat anionic trypsin (*42*) as well as BPTI in complex with human mesotrypsin and human cationic trypsin (*33*). To further understand these biochemically important interactions, we have studied the kinetic mechanisms of inhibition of the serine proteinases, FXIa and trypsin by the Kunitz inhibitors, PN2KPI and BPTI.

PN2KPI and BPTI are structurally very similar Kunitz inhibitory protein family members, each of which has six conserved cysteine residues making three intrachain disulphide bonds resulting in stable compact structures containing two loop regions that interact with the proteases. X-ray crystal structures of these inhibitory proteins have been solved in complex with several serine proteases such as trypsin, chymotrypsin and the catalytic domain of FXIa (*28*, *41*, *42*). Structural data from X-ray crystallography reveal similar superimposable backbone structures except for a small region from residues 39–41 (*43*). The current study compares these structurally homologous inhibitors, PN2KPI and BPTI, and contrasts their biochemical properties in the inhibition of the structurally similar serine proteinases, human FXIa and bovine trypsin. We further demonstrate, by using P1 site swap mutants, PN2KPI-R15 K and BPTI-K15 R, that the P1 site residues of the inhibitors are responsible in part for the functional differences in their enzyme specificities.

Experimental Procedures

Native and mutant inhibitor gene constructs for Pichia pastoris expression

The PN2KPI domain was amplified by polymerase chain reaction (PCR) from the full-length human PN2 gene as previously described (*28*). PCR-based site-directed mutagenesis (QuikChange, Strategene, USA) was utilized to introduce an Arg to Lys mutation at the P1 site and Ala mutations (PN2KPI-P13A, R15A, M17A, S19A, R20A and F34A) as explained in detail elsewhere (*28*). Utilizing a similar approach BPTI was obtained as a 206-bp PCR amplification product from bovine liver cDNA (Biochain Institute, Inc., USA) and ligated into a yeast expression vector, pPICZαA (Invitrogen, USA) and the BPTI P1 site was mutated from Lys to Arg (BPTI-K15 R) by inserting the codon preferentially used in yeast. The pPICZαA plasmids containing native and mutant inserts were sequenced from 5′ to the α-mating factor secretion signal using an AOX5 primer to confirm the mutations at the desired sites as well as the reading frame integrity.

Native and mutant protein expression in yeast cells

As explained in detail elsewhere for PN2KPI (*28*), the pPICZαA plasmid containing PN2KPI, BPTI and respective mutant gene constructs were incorporated into the methylotrophic yeast *Pichia pastoris* X33 competent cell genome (Invitrogen, USA) by recombinational cloning. Zeocin selected yeast clones were lysed either by lyticase (Sigma, USA) or by repeated freeze-thaw cycles. The lysates were checked by PCR using respective gene specific forward and reverse primers for correct insert size. Successful clones were propagated in buffered medium containing glycerol and yeast nitrogen base (BMGY) and expressed in buffered medium containing methanol and yeast nitrogen base (BMMY) for 96 h at 30°C under vigorous agitation, supplemented with 0.5% methanol every 24 h.

Purification of recombinant Kunitz inhibitory domain proteins

Purification of recombinant PN2KPI and its mutant protein followed the protocol explained earlier (*28*). For BPTI and BPTI-K15 R purification certain modifications were made as explained below. *Pichia pastoris* BMMY cultures containing secreted proteins were centrifuged to remove yeast cells. The supernatant was precipitated using saturating concentrations of ammonium sulphate and centrifuged at 11,000*g* for 30 min. Pellets were resuspended in 50 mM Tris buffer, pH 7.8 and the proteins were purified using desalting columns (G25 16/60, Amersham Biosciences Corp., USA) followed by ion exchange chromatography (10–20 ml SP HP columns, Amersham Biosciences Corp., USA) in 50 mM Tris buffer pH 7.8 and eluted with sodium chloride. The eluted samples were concentrated in dialysis tubing (Float-a-lyser, Spectrum Laboratories, Inc., USA) using an external dehydrant, cross-linked sodium polyacrylate gel (Spectragel; Spectrum Laboratories, Inc., USA), at 4°C. Concentrated samples were size fractionated using size-exclusion columns (HiLoad 30, 16/60, Amersham Biosciences Corp., USA) in 150 mM NaCl, 50 mM Tris buffer, pH 7.8 (TBS).

The concentrations of purified proteins were estimated either by the bicinchoninic acid assay (Pierce Biotechnology, Inc., USA) or from their extinction coefficient, 5960 $M^{-1}\,cm^{-1}$ at 280 nM, estimated from the protein sequence (ProtParam, ExPASy, Swiss Institute of Bioinformatics). The yields of various preparations of PN2KPI and mutants were 0.7–10 $mg\,l^{-1}$, whereas those of BPTI and BPTI-K15 R were 1–3.5 $mg\,l^{-1}$ of culture volume. On silver-stained SDS–PAGE gels under reducing conditions, the purified proteins were single, sharp bands at 6.3–6.5 kDa (data not shown) and probed by western blotting using rabbit anti-Alzheimer's β-amyloid protein precursor polyclonal antibody (Chemicon International, USA) for PN2KPI.

Measurement of initial rates of S-2366 hydrolysis by FXIa

Increasing concentrations of S-2366 (L-pyro-Glu-Pro-Arg-*p*-nitroanilide-HCl; 0-2 mM) in 15 µl of 50 mM Tris, 150 mM NaCl, 5 mM $CaCl_2$, 0.1% BSA, pH 7.6 (TBSB) was placed in the wells of a 96-well microplate to which 135 µl of premixed and preincubated (30 min) enzyme/inhibitor mixture in TBSB was added. The final concentration of the FXIa (Haematologic Technologies Inc., VT, USA) in the reaction mixture was 1 nM. Generation of the product pNA was monitored by measuring absorbance at 405 nM in a microplate reader for 10 min at 37°C. Initial velocity measurements were analyzed using KaleidaGraph v3.5 nonlinear regression software.

Determination of equilibrium inhibition constant (K_i)

To establish K_i values for the inhibition FVIIa, FIXa, FXa, plasmin (all from Haematologic Technologies Inc., VT, USA), thrombin, FXIIa, plasma kallikrein (all from Enzyme Research Laboratories, IN, USA) and trypsin by PN2KPI, BPTI and their mutants, assays were carried out in 50 mM Tris, 150 mM NaCl, 0.1% BSA, pH 7.5 buffer (TBSB) using appropriate chromogenic or fluorogenic substrates to measure residual activity after incubation with the Kunitz inhibitors. The final enzyme concentrations used were

thrombin (1 nM), FVIIa (5 nM or 50 nM in the presence or absence, respectively, of 50 nM tissue factor, obtained from Calbiochem, CA,USA), FIXa (50 nM), FXa (1 nM), FXIIa (25 nM), plasmin (10 nM) or plasma kallikrein (1 nM) in 135 µl volume for 30 min at 37°C in a microtitre plate to establish equilibrium between the inhibitor and the enzyme. To this preincubation mixture, 15 µl of substrate was added to the final reaction volume of 150 µl. The substrates (all obtained from Chromogenix, DiaPharma Group, Inc., OH, unless otherwise indicated) and their final concentrations for the reactions were: 200 µM of S-2366 (L-pyroGlu-Pro-Arg-pNA-HCl) for thrombin; 2000 µM of Chromozyme t-PA (CH_3-SO_2-D-Phe-Gly-Arg-pNA; Roche Diagnostics, IN, USA) for FVIIa; 3000 µM of Spectrozyme-FIXa ($MeSO_2$-D-CHG-Gly-Arg-pNA.AcOH; American Diagnostica Inc., CA, USA) for FIXa; 400 and 80 µM of S2765 (N-α-Z-D-Arg-Gly-Arg-pNA.2HCl) for FXa and trypsin, respectively; 250 or 300 µM of S2302 (Pro-Phe-Arg-pNA.2HCl) for FXIIa or plasma kallikrein, respectively; and 400 µM of S2403 (pyroGlu-Phe-Lys-pNA.HCl) for plasmin. The substrate concentrations used were at or above their determined K_m values for their respective enzymes. The initial reaction velocities of chromogenic substrate cleavage, determined for 10–15 min at 37°C in a microplate reader at 37°C (Thermomax, Molecular Devices, USA) were converted to fraction of amidolytic activity remaining. For fluorogenic assays increasing concentrations of PN2KPI, BPTI and mutants in TBSB, were incubated with FXIa (25 pM) in 90 µl volumes for 30 min at room temperature in black polystyrene microtitre plates (Corning, NY, USA) to establish equilibrium between the inhibitor and the enzyme. To this preincubation mixture, 10 µl of the fluorogenic substrate, Boc-Glu(OBzl)-Ala-Arg-methylcoumarin acetate (Boc-EAR-MCA; Peptides International, Inc., Louisville, Kentucky) was added to a 275 µM final concentration in a total reaction volume of 100 µl. For studies with trypsin, increasing concentrations of PN2KPI (0–0.7 nM), or BPTI (0–2.8 nM) in TBSB were incubated with 100 pM trypsin (bovine source, Sigma, St Louis, Missouri) in 90 µl volume for 30 min at room temperature to establish equilibrium between the inhibitor and the enzyme. Ten microlitres of the fluorogenic substrate Boc-EAR-MCA was added to a final concentration of 6 µM in a total reaction volume of 100 µl. The progress of hydrolysis was monitored at an emission wavelength (Em_{440}) of 440 nm after excitation at 350 nm (Ex_{350}). The fluorimetric initial reaction velocity readings for 10–15 min in a microplate reader at room temperature (Spectramax M2, Molecular Devices, USA) were converted to fraction of amidolytic activity remaining. In both colorimetric and fluorescence assays, the IC_{50} values were determined by plotting residual enzyme activity against inhibitor concentration using KaleidaGraph v3.5 software and K_{ieq} were calculated using the equation explained in 'Data analyses' section.

Progress curve generation

Release of a highly fluorescent product from the peptidyl substrate Boc-EAR-MCA by FXIa or trypsin was monitored in the presence of varying concentrations of PN2KPI or BPTI. The values of K_m for Boc-EAR-MCA hydrolysis by FXIa and trypsin were determined to be 275 and 1.2 µM, respectively. Substrate hydrolysis was initiated by the addition 10 µl of enzyme (25 pM FXIa or 1 nM trypsin, final concentrations) to 90 µl of a mixture of inhibitor (varying concentrations) and fluorogenic substrate in TBSB in 96-well black polystyrene microtitre plates. The progress of substrate hydrolysis was monitored for up to 50 min at 15- or 60 s intervals at room temperature (ranging from 24°C to 27°C) in a fluorescence plate reader as described earlier. In order to study whether trypsin inhibition by BPTI follows irreversible inhibition kinetics, progress curves of substrate hydrolysis were generated using final concentrations of trypsin (1 nM), BPTI (16 nM) and varying concentrations (1.2–12 µM) of fluorogenic substrate (*44*). The progress of fluorogenic substrate hydrolysis was monitored for 50 min at room temperature.

Data analyses

For other than the tight binding inhibitors, values of K_{ieq} were derived from their IC_{50} using the following equation:

$$K_{ieq} = \frac{IC_{50}}{(1 + \{[S]/K_m\})} \qquad (1a)$$

where, [*S*] is substrate concentration, K_m is the Michaelis constant.

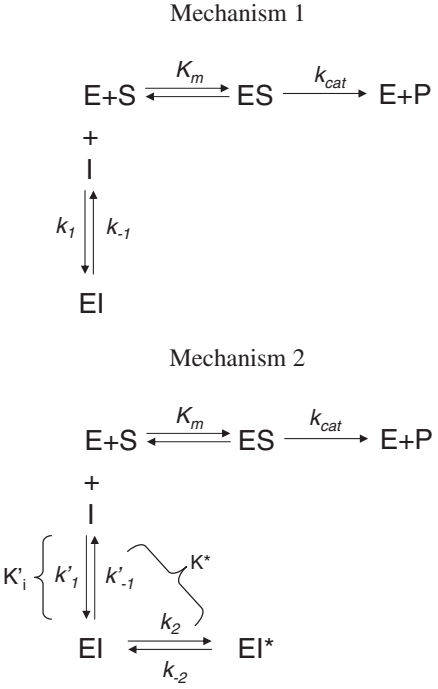

Fig. 1 Enzyme inhibition mechanisms. In mechanism 1, the binding of inhibitor and isomerization of the complex are simultaneous and not distinguishable and therefore, k_1 and k_{-1} represent the overall on-rate and off-rate constants. In mechanism 2, on the other hand, inhibition of enzyme occurs in two steps, characterized by the formation of a loose EI complex described by rate constants k'_1 and k'_{-1} and isomerization of EI–EI* (the stable complex) occurs with an on-rate of k_2 and an off-rate of k_{-2}.

For tight-binding inhibitors the K_{ieq} were calculated using the following equation (*45*):

$$V_s = V_o \frac{K_{ieq}(1 + [S]/K_m)}{I + K_{ieq}(1 + [S]/K_m)} \qquad (1b)$$

where V_s is the velocity after a steady state has been reached between enzyme and inhibitor, V_o is the velocity of product formation at the start of the reaction, K_{ieq} represents the equilibrium inhibition constant, [*S*] is substrate concentration, K_m is the Michaelis constant and *I* is the inhibitor concentration.

Inhibition by slow, tight-binding inhibitors can be described by two general mechanisms (*46–49*) as depicted in Fig. 1. In mechanism 1, the formation of the final tight enzyme–inhibitor complex occurs slowly but directly without any substantial accumulation of an initial loose complex. In this mechanism, k'_1 and k'_{-1} are the second- and first-order kinetic rate constants. In mechanism 2, there is accumulation of an initial enzyme-inhibitor complex with an inhibition constant of K'_i that isomerizes in a second step to form the tight complex and both k_2 and k_{-2} are first-order kinetic constants.

A general equation for progress curves for slow-binding inhibition is given by the following equation:

$$P = V_s t + (V_o - V_s)(1 - e^{-k_{obs} t})/k_{obs} \qquad (2)$$

where V_o is the velocity of product formation at the start of the reaction, V_s is the velocity after a steady state has been reached between enzyme and inhibitor, k_{obs} is the observed first order rate constant that characterizes the transition from initial velocity to steady state velocity and *P* is the concentration of product formed at time *t*.

Kinetic parameters K_m and k_{cat} for substrate hydrolysis in the presence of the inhibitor are related to V_o and k_{obs} as follows:
Mechanism 1

$$V_o = \frac{(k_{cat} E_T S_0)}{(K_m + S_0)}, \qquad k_{obs} = k_{-1} + \frac{k_1 I_T}{1 + S_0/K_m} \qquad (2a)$$

Thus, if enzyme inhibition occurs involving mechanism 1 the initial velocity would be independent of the inhibitor concentration and k_{obs} versus I would be linear with an y-intercept of k_{-1}.

Mechanism 2

$$V_o = \frac{k_{cat} E_T S_0}{K_m((1 + I_T/K_i') + S_0)}$$
$$k_{obs} = k_{-2} + \frac{k_2 I_T}{K_i'(1 + S_0/K_m) + I_T} \quad (2b)$$

where, E_T and I_T are total concentrations of enzyme and inhibitor, respectively, and S_0 is substrate concentration.

Thus, for inhibition by mechanism 2, V_o is inversely related to the inhibitor concentration and k_{obs} versus I is hyperbolic. Therefore, by analyzing how V_o and k_{obs} are related to the inhibitor concentration one may assess whether the enzyme inhibition is a single step (mechanism 1) or a two-step (mechanism 2) phenomenon.

KaleidaGraph (v3.5) was used for obtaining values of V_o, V_s and k_{obs}. Values of k_{-1} (mechanism 1) or k_{-2} (mechanism 2) were derived from progress curves by using the following relationship (*45*, *49*):

$$k_{-1} \text{ or } k_{-2} = k_{obs} \frac{V_s}{V_o} \quad (3)$$

The second-order rate constant k_1 (mechanism 1) was then obtained from the following linear equation:

$$k_{obs} = k_{-1} + (k_1 I)/\{1 + [S]/K_m\} \quad (4)$$

Calculated K_i (K_{ical}) is thus given by k_{-1}/k_1.

To determine whether trypsin forms a non-dissociable complex with BPTI under our experimental conditions, we generated progress curves using fixed enzyme and inhibitor concentrations while varying the substrate concentration. Product formation approaches a finite value [P_∞] with progress of time and this value decreases with decrease of substrate concentration represented by the following equation (*44*):

$$[P_\infty] = \frac{V([S]/K_m)}{(1 + ([S]/K_m))k_{1app} I} \quad (5)$$

where V is the rate of hydrolysis of substrate in the absence of inhibitor, [S] is the substrate concentration, K_m is the Michaelis constant, $k_{1\,app}$ represents the apparent association rate constant of the enzyme–inhibitor complex in the presence of the substrate and I is the inhibitor concentration. From the values of $k_{1\,app}$ at different substrate concentrations, the association rate constant k_1 for formation of trypsin–BPTI complex was calculated using the following equation:

$$\frac{1}{k_{1\,app}} = \frac{1}{k_1} + \frac{[S]}{(k_1 K_m)} \quad (6)$$

The intercept of the plot of $1/k_{1\,app}$ versus [S] represents $1/k_1$.

Results

Inhibition of coagulation proteases and trypsin by PN2KPI

Initial studies were aimed at determining the specificity of interactions of PN2KPI with a variety of coagulation enzymes and trypsin (Supplementary Fig. S1 and Table I). FXIa and trypsin were inhibited with K_i values of 0.81 nM and 0.03 nM, respectively, whereas no evidence of thrombin inhibition was observed, and the K_i values for FVIIa (in the absence and presence of tissue factor) FIXa, FXa, FXIIa and plasmin were all >400 nM, whereas kallikrein was inhibited by PN2KPI with a K_i value of 183 nM.

Structural comparisons of PN2KPI and BPTI

The primary structures of the highly homologous Kunitz inhibitors PN2KPI and BPTI are shown in Fig. 2A. For comparison of three-dimensional structures, we superimposed the PN2KPI X-ray crystal structure from the PN2KPI-FXIa catalytic domain complex (PDB:1ZJD) (*28*) and the BPTI structure from the BPTI–trypsin complex (PDB: 2FTL) (*29*). The crystal structures of these two proteins were superimposable, displaying a striking similarity of the main-chain conformations of PN2KPI and BPTI. The two subdomains within these inhibitors termed loops 1 and 2 (Fig. 2B) that interact most closely with their cognate proteinases are highly homologous sharing primary sequence identity of 70% and 83%, respectively between PN2KPI and BPTI (Fig. 2A). A short sequence of ascending residues, 39–41, adjacent to loop 2 displays some backbone deviation between the two inhibitors (Fig. 2B). However, this sequence of residues does not interact with the cognate proteinases as observed from the crystal structures of the enzyme–inhibitor complexes.

Inhibition of FXIa, kallikrein, plasmin and trypsin by PN2KPI mutants

Based on an inspection of the X-ray crystal structure of the PN2KPI/FXIa complex (*28*), we have selected several key residues in PN2KPI for mutational analysis to determine the effects on inhibition of FXIa, plasmin, kallikrein and trypsin (Table II), the proteases most susceptible to inhibition by PN2KPI, according to our results (Table I). The PN2KPI-R15A lost virtually all its inhibitory activity against all four proteases, confirming the essential role of the P1 residue of the Kunitz inhibitor in protease inhibition. Interestingly, the PN2KPI-M17A mutant displayed ~25-fold gain of function against kallikrein without any significant change in K_i values for FXIa, plasmin or trypsin. Whereas we observed a significant loss of activity for PN2KPI-P13A, PN2KPI-R20A and PN2KPI-F34A mutants in the inhibition of FXIa, kallikrein and plasmin, there was no significant effect of any of these mutants in trypsin inhibition.

Equilibrium inhibition of FXIa and trypsin by PN2KPI and BPTI and P1 site mutants

To determine values of K_i for inhibition of FXIa and trypsin by PN2KPI and BPTI (Supplementary Fig. S2), the inhibitors were preincubated with the enzyme for 30 min at room temperature, and the residual enzyme activity was determined. The K_i value (Table III) for PN2KPI inhibition of FXIa was 0.81 ± 0.31 nM (Supplementary Fig. S2A), consistent with previous reports (*18–24*) indicating that PN2 is a tight-binding inhibitor of FXIa. In contrast, the K_i for inhibition of FXIa by BPTI determined by the equilibrium method was 627 nM (Supplementary Fig. S2B) demonstrating that in spite of the striking similarity in three-dimensional structure, the affinity of PN2KPI for FXIa is ~775-fold tighter than that of BPTI for FXIa. To examine the contribution of the P1 residue of the two Kunitz- type inhibitors on the inhibition of FXIa, we prepared two mutant proteins PN2KPI-R15 K (mimicking BPTI at the P1 site) and BPTI-K15 R (mimicking PN2KPI at the P1 site). These P1 site

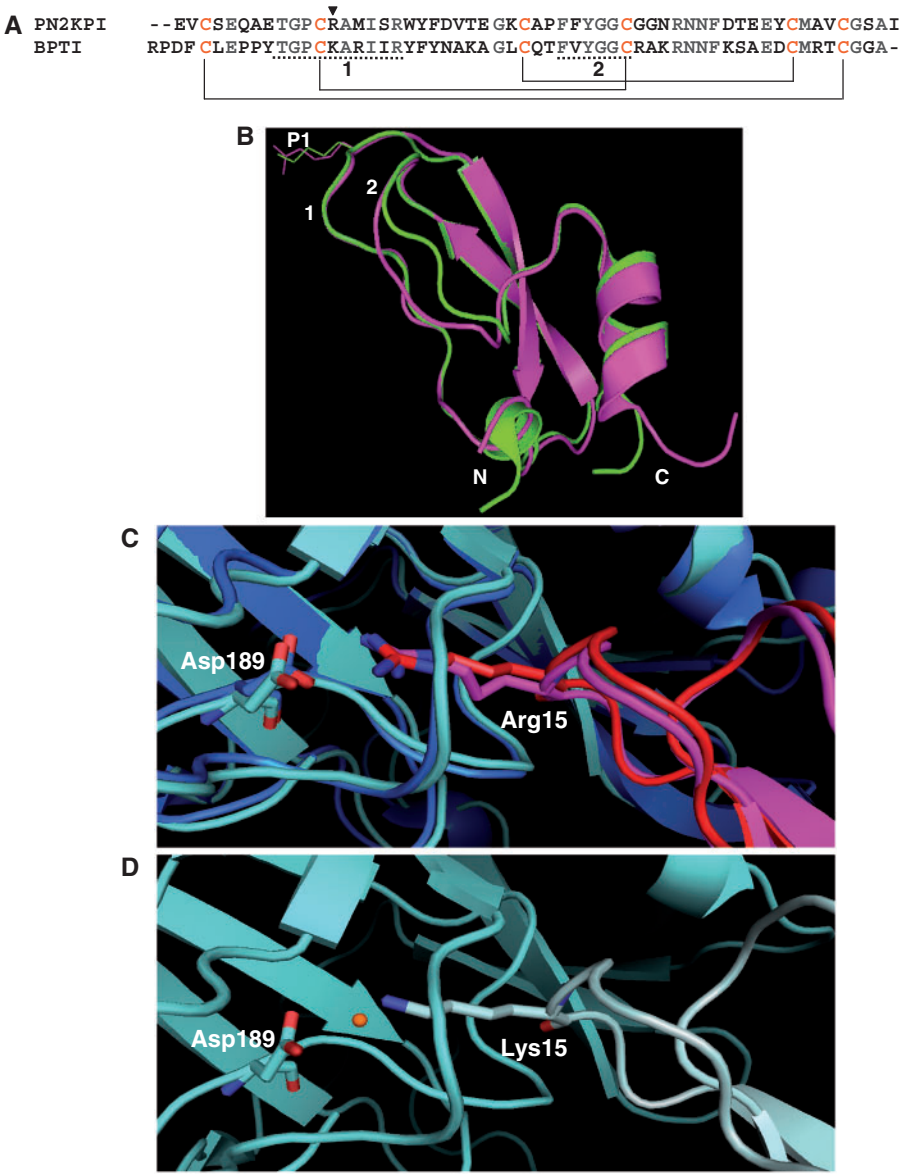

Fig. 2 The primary and tertiary structures of the Kunitz-type inhibitors, PN2KPI and BPTI (A and B) and comparison of interactions of P1 site residues Arg[15] and Lys[15] (of PN2KPI and BPTI, respectively) with the Asp[189] of FXIa catalytic domain and Trypsin (C and D). (A) The primary amino acid sequence of PN2KPI and BPTI. The P1 site residue is shown with an arrowhead. Underlined sequences are the enzyme interacting loops 1 and 2 of the inhibitor, which share a sequence identity of 70% and 83%, respectively. Cysteine residues that make intrachain disulfide bonds are shown in yellow and disulfide bonds are shown in solid lines. (B) Superimposed X-ray crystal structures of PN2KPI (in pink, PDB: 1ZJD) and BPTI (in green, PDB: 2FTL) shown with P1 site residues Arg[15] and Lys[15] side chains. Loops 1 and 2, and N and C terminals are indicated. (C) PN2KPI in complex with FXIa catalytic domain (dark blue; PDB:1ZJD) and trypsin (light blue; PDB:1TAW). Arg[15] of PN2KPI (pink and red) protrudes into the S1 specificity pocket of the catalytic domain of FXIa and trypsin to establish a salt bridge with Asp[189]. (D) Lys[15] of BPTI (grey) protrudes similarly into the S1 specificity pocket of trypsin (light blue; 2FTL) to establish a hydrogen bond with Asp[189], with the intervention of a water molecule (orange).

Table I. Inhibition of coagulation proteases by PN2KPI.

Enzyme	FIIa	FVIIa	FVIIa+TF	FIXa	FXa	FXIa	FXIIa	Plasmin	Kallikrein	Trypsin
K_i [nM]	NI[a]	3,500	756	5,500	1,150	0.81	7,610	459	183	0.03

[a]No inhibition observed at the highest inhibitor concentration (8 μM).

mutants PN2KPI-R15 K (Supplementary Fig. S2C) and BPTI-K15 R (Supplementary Fig. S2D) were characterized by K_i values in FXIa inhibition of 11.3 nM and 4.1 nM, respectively (Table III). In marked contrast, the K_i values for trypsin inhibition by PN2KPI (Supplementary Fig. S2E), BPTI (Supplementary Fig. S2F), PN2KPI-R15 K (Supplementary Fig. S2G) and BPTI-K15 R (Fig. S2H), ranging between 0.016 and 0.076 nM (Table III), were not significantly different biologically.

Progress curve analysis of FXIa and trypsin inhibition

To investigate the mechanisms by which PN2KPI and BPTI inhibit FXIa and trypsin, progress curves generated in the absence and presence of various inhibitor concentrations were analysed**.** The progress curves for FXIa inhibition by PN2KPI (0–32 nM) and by BPTI (0–5 μM) were monitored at 15–60-s intervals for a maximum duration of 50 min. FXIa inhibition displayed distinct progress curve patterns for inhibition by PN2KPI (Fig. 3A) and BPTI (Fig. 5A). In the case of inhibition of FXIa by PN2KPI (Fig. 3A), PN2KPI-R15 K (Fig. 4A) and BPTI-K15 R (Fig. 6A) the initial rates of fluorogenic substrate hydrolysis were independent of inhibitor concentration, and the progress curves demonstrated progressive decreases with increasing inhibitor concentration. On the contrary, the initial rates of inhibition of FXIa by BPTI were linear at all inhibitor concentrations and the slopes were progressively decreased with increasing concentrations of BPTI (Fig. 5A). Similarly, the progress curves of trypsin inhibition by PN2KPI and BPTI (Figs 7A and 8A) demonstrated initial rates that were independent of inhibitor concentrations as were found for FXIa inhibition by PN2KPI. These data demonstrate that FXIa inhibition by PN2KPI and trypsin inhibition by BPTI both conform to mechanism 1 with slow, single-step equilibration between enzyme and inhibitor.

In secondary plots, values of k_{obs} obtained from progress curves using equation (*2*) were plotted as a function of the corresponding inhibitor concentrations. A linear relationship of k_{obs} versus inhibitor concentration was observed for PN2KPI (Fig. 3B), PN2KPI-R15 K (Fig. 4B) and BPTI-K15 R (Fig. 6B). In all these cases, inhibition of FXIa conforms to mechanism 1 (Fig. 1 and Table III), which takes place in a single step involving the gradual formation of a tight complex. In contrast, BPTI inhibition of FXIa follows simple steady-state kinetics with the rate of substrate hydrolysis remaining the same throughout the time period at each inhibitor concentration and progressively lower rates observed with progressive increases in inhibitor concentration (Fig. 5A). This is shown in a separate confirmatory assay (Fig. 5B) in which titration curves of chromogenic substrate (S-2366) hydrolysis by FXIa in the presence of varying concentrations of BPTI demonstrated increasing values of K_m without any alteration of V_{max}, indicative of pure competitive inhibition (Table I). Similar to FXIa inhibition, trypsin inhibition by PN2KPI also displays a single step inhibition process displaying a linear relationship of k_{obs} versus inhibitor concentration (Fig. 7B).

Progress curves of trypsin inhibition by BPTI (Fig. 8A) demonstrate unequivocally that the initial rates of trypsin inhibition were independent of BPTI concentration suggesting that the inhibition conforms to mechanism 1. However, we were unable to obtain reliable k_{obs} values from these progress curves possibly because of the extremely slow rate of dissociation of the enzyme–inhibitor complex. Indeed Zhou *et al.* (*44*) demonstrated that trypsin inhibition by BPTI follows apparently irreversible kinetics with an association rate constant of $0.37 \times 10^6\ M^{-1}\ s^{-1}$. Vincent and Lazdunski (*50*) reported the first-order rate constant of dissociation of the same inhibition reaction to be $6.6 \times 10^{-8}\ s^{-1}$. We attempted to generate progress curves for the dissociation of the complex, but even at the end of 60 min free trypsin liberated was <1% (data not shown). This fact together with the slow loss of activity of trypsin on standing in solution beyond 60 min as observed from chromogenic or fluorogenic substrate hydrolysis made it impossible to generate the data required for calculation of the relevant rate constants. We therefore aimed to determine whether trypsin forms a non-dissociable complex with BPTI under our experimental conditions, which are significantly different from those used previously (*44*). For this purpose, we generated progress curves using fixed enzyme and inhibitor concentrations while varying the substrate concentration (Fig. 8B). It is apparent

Table II. Inhibition of FXIa, plasma kallikrein, plasmin and trypsin by PN2KPI mutants[a].

	K_i [nM]			
Inhibitors	**FXIa**	**Kallikrein**	**Plasmin**	**Trypsin**
PN2KPI	0.81	183	459	0.03
PN2KPI-P13A	2.96	1005	2,690	0.048
PN2KPI-R15A	NI[b]	NI[b]	NI[b]	NI[b]
PN2KPI-M17A	0.81	7.4	479	0.054
PN2KPI-S19A	0.93	253	615	0.024
PN2KPI-R20A	2.83	6,320	914	0.041
PN2KPI-F34A	4.92	398	2,640	0.088

[a]Trypsin data represent fluorogenic assay results, whereas the results for the rest of the enzymes are based on chromogenic assays.
[b]No inhibition observed at inhibitor concentrations up to 4 μM.

Table III. Kinetic studies for inhibition of FXIa and trypsin by Kunitz inhibitors.

Enzyme	**Inhibitor**	**Mechanism**	K_{ieq} [nM]	$k_1\ M^{-1}\ s^{-1}$	$k_{-1}\ s^{-1}$	K_{Ical} [nM]
FXIa	PN2KPI	1	0.81 ± 0.3	0.24×10^6	3.2×10^{-4}	1.3
	PN2KPI-R15 K	1	11.3 ± 0.6	1.7×10^5	3.1×10^{-3}	18.2
	BPTI	Competitive	627 ± 9.1			708 ± 81[a]
	BPTI-K15 R	1	4.1 ± 0.3	2.87×10^5	2.3×10^{-3}	8.01
Trypsin	PN2KPI	1	0.03 ± 0.007	3.4×10^6	3.7×10^{-4}	0.049
	PN2KPI-R15 K		0.047 ± 0.003			
	BPTI	1	0.072 ± 0.001	4.4×10^5	3.2×10^{-5}	
	BPTI-K15 R		0.016 ± 0.002			

[a]Calculated from Michaelis–Menten plot represented in Fig. 5B.

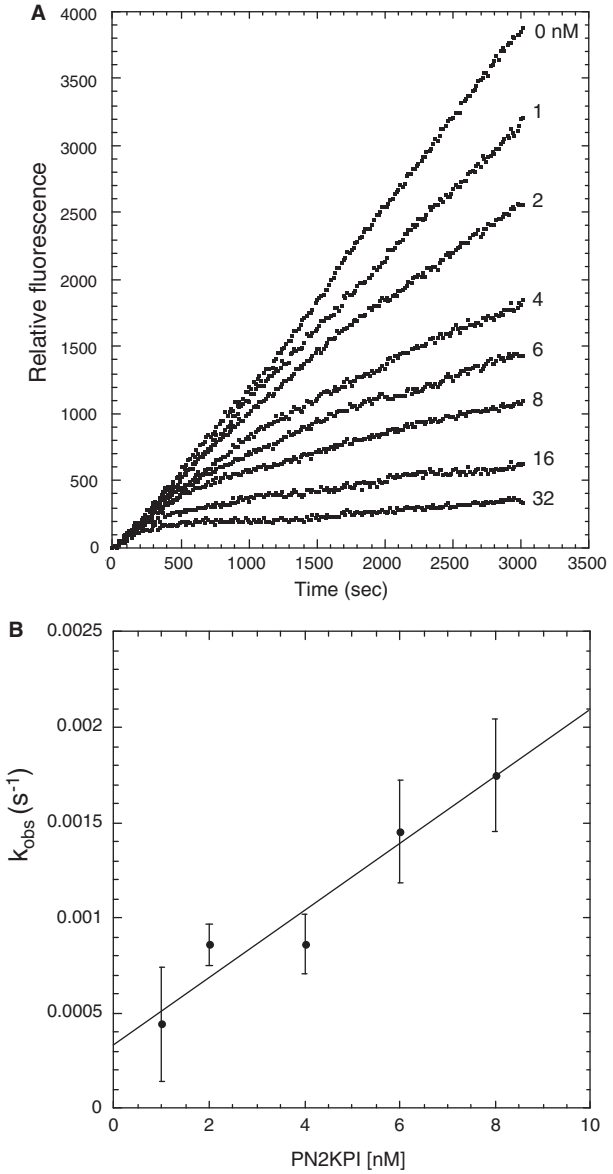

Fig. 3 Progress curve of fluorogenic substrate (Boc-EAR-MCA) hydrolysis by FXIa in the presence of PN2KPI and the secondary plot. (A) Hydrolysis of Boc-EAR-MCA (275 μM) by FXIa (25 pM) in the presence of varying concentrations of PN2KPI (0–32 nM) were monitored for 3,000 s. Inhibitor concentrations used are shown on the right, adjacent to the respective curve. (B) Secondary plot of k_{obs} values versus PN2KPI concentration. The values of k_{obs} were obtained by fitting progress curve data shown in Figure (A) using equation (*2*). The k_{obs} (s^{-1}) values for each inhibitor concentration were calculated from the averaged values (± SEM) of three assays each done in duplicate. All assays were background subtracted with substrate autolysis for the entire assay duration.

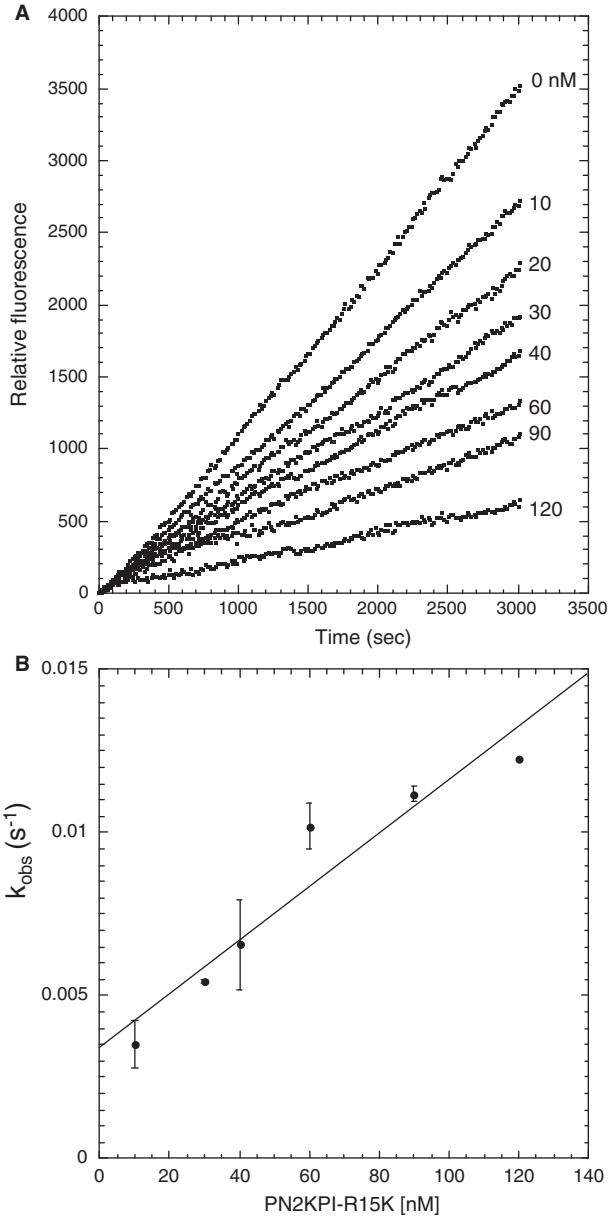

Fig. 4 Progress curve of fluorogenic substrate (Boc-EAR-MCA) hydrolysis by FXIa in the presence of PN2KPI-R15 K and the secondary plot. (A) Hydrolysis of Boc-EAR-MCA (275 μM) by FXIa (25 pM) in the presence of varying concentrations of PN2KPI-R15 K (0–120 nM) were monitored for 3,000 s. Inhibitor concentrations used are shown on the right, adjacent to the respective curve. (B) Secondary plot of k_{obs} values versus PN2KPI-R15 K concentration. The k_{obs} (s^{-1}) values for each inhibitor concentration were calculated from the averaged values (± SD) of three assays each done in duplicate. All assays were background subtracted with substrate autolysis for the entire assay duration.

from these results that product formation approaches a finite value [P_∞] with progress of time and that this value decreases with decrease of substrate concentration. These results confirm the previous conclusion that trypsin inhibition by BPTI is non-dissociable (*44*). From progress curves shown in Fig. 8B we could obtain the values of $k_{1\,app}$ (the apparent association rate constant of the enzyme–inhibitor complex in the presence of the substrate) using equation (*6*). The value of the association rate constant k_1 ($4.4 \times 10^5\,M^{-1}\,s^{-1}$) of trypsin-BPTI complex formation was then obtained from the intercept of the secondary plot of $1/k_{1app}$ versus [S] shown as an inset in Fig. 8B. The dissociation rate constant k_{-1} ($3.2 \times 10^{-5}\,s^{-1}$) shown in Table III was obtained assuming $K_{i\,eq} = k_{-1}/k_1$.

Discussion

Factor XI (FXI) is the precursor of a plasma serine protease formed by factor XIIa or thrombin that

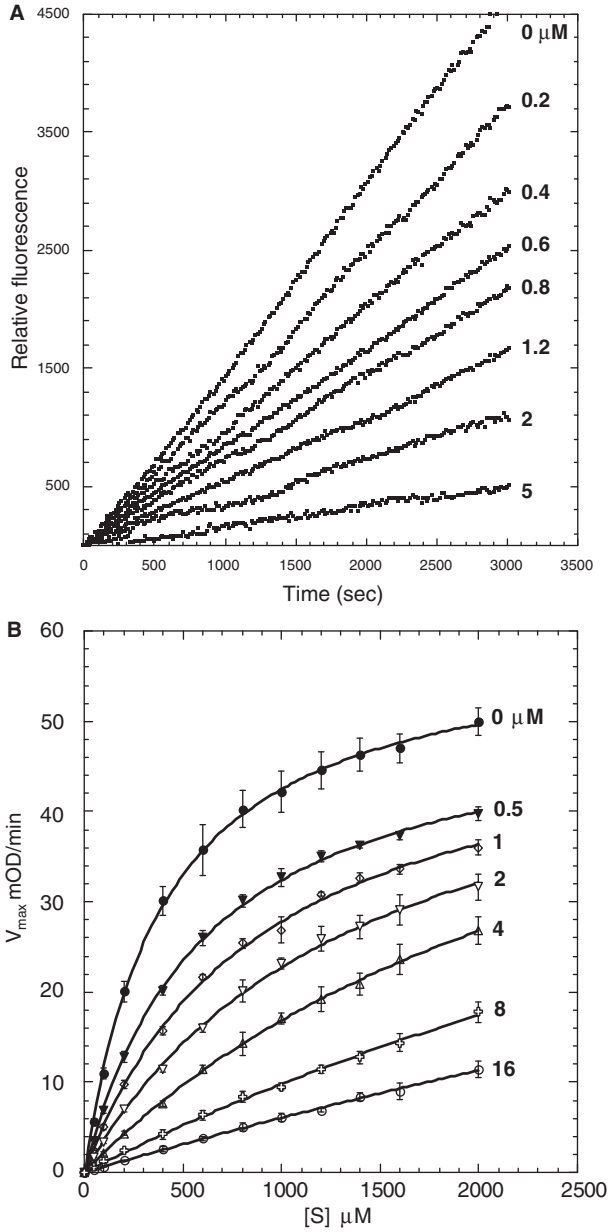

Fig. 5 Progress curve of fluorogenic substrate (Boc-EAR-MCA) hydrolysis by FXIa in the presence of BPTI. (A) Hydrolysis of Boc-EAR-MCA (275 μM) by FXIa (25 pM) in the presence of varying concentrations of BPTI (0–5 μM) were monitored for 3,000 s. Inhibitor concentrations used are shown on the right, adjacent to the respective curve. (B) S-2366 hydrolysis by FXIa (1 nM) in the presence of varying concentrations of BPTI. Michaelis–Menten titration curves of initial rates as a function of substrate concentration were generated as described in the 'Experimental procedures' section. Each data point represents the mean (± SD) of two to four assays each done in duplicate.

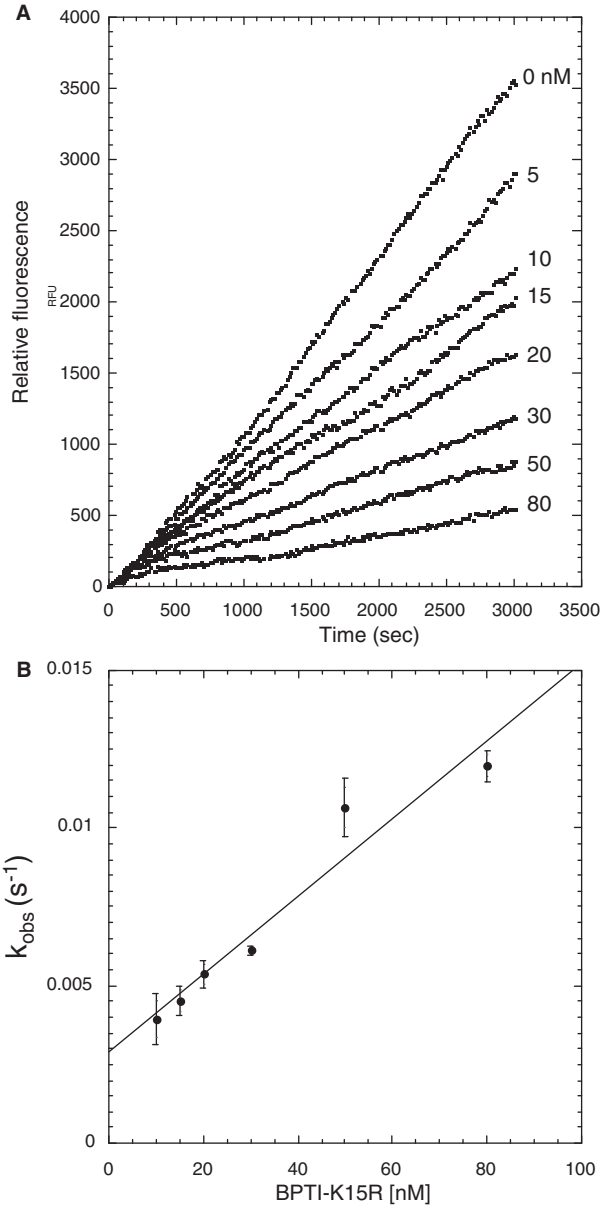

Fig. 6 Progress curve of fluorogenic substrate (Boc-EAR-MCA) hydrolysis by FXIa in the presence of BPTI-K15 R. (A) Hydrolysis of Boc-EAR-MCA (275 μM) by FXIa (25 pM) in the presence of varying concentrations of BPTI-K15 R (0–80 nM) were monitored for 3,000 s. Inhibitor concentrations used are shown on the right, adjacent to the respective curve. (B) Secondary plot of k_{obs} values versus BPTI-K15 R concentration. The k_{obs} (s^{-1}) values for each inhibitor concentration were calculated from the averaged values (± SD) of three assays each done in duplicate.

participates in the consolidation phase of blood coagulation and is implicated in pathological thrombosis, rendering it a potential target for the development of antithrombotic agents. As the Kunitz-type inhibitor, protease nexin-2 (PN2-KPI) is a potent inhibitor of FXIa, the major question addressed in the present study is the physiological relevance, specificity and mechanism of action of the platelet α-granular protein, PN2/AβPP. Previous studies from our laboratory indicate that the major interactions required for FXIa inhibition by PN2 are localized to the catalytic domain of FXIa and the KPI domain of PN2 (*24*). We have also found that secretion of PN2 from activated platelets limits the lifetime of FXIa activity within the locus of activated platelets. However, in the presence of activated platelets, HK and Zn^{2+} ions, FXIa bound to the surface of activated platelets is protected from inactivation by PN2KPI (*23*, *51*).

It has been demonstrated (*52*) that over-expression of PN2/AβPP in circulating platelets of transgenic mice was associated with inhibition of thrombosis

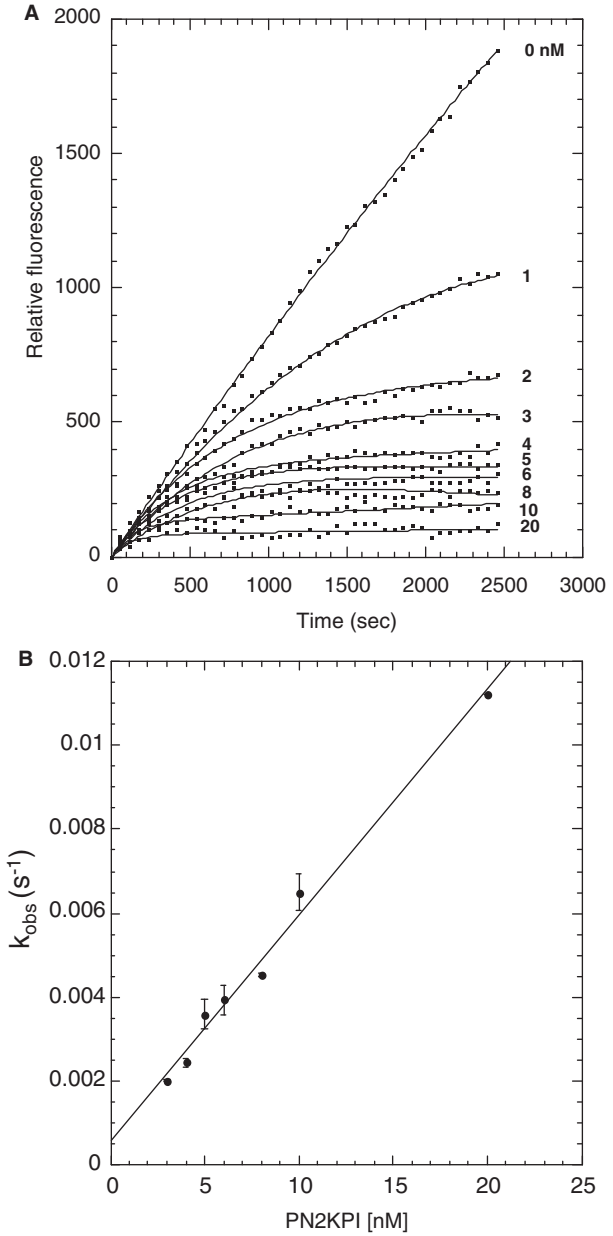

Fig. 7 Progress curve of fluorogenic substrate (Boc-EAR-MCA) hydrolysis by trypsin in the presence of PN2KPI and the secondary plot. (A) Hydrolysis of Boc-EAR-MCA (6 μM) by trypsin (0.5 nM) in the presence of varying concentrations of PN2KPI (0–20 nM) were monitored for 2,500 s. Inhibitor concentrations used are shown on the right, adjacent to the respective curve. (B) Secondary plot of k_{obs} values versus PN2KPI concentration. The k_{obs} (s^{-1}) values for each inhibitor concentration were calculated from the averaged values (± SD) of five assays each done in duplicate.

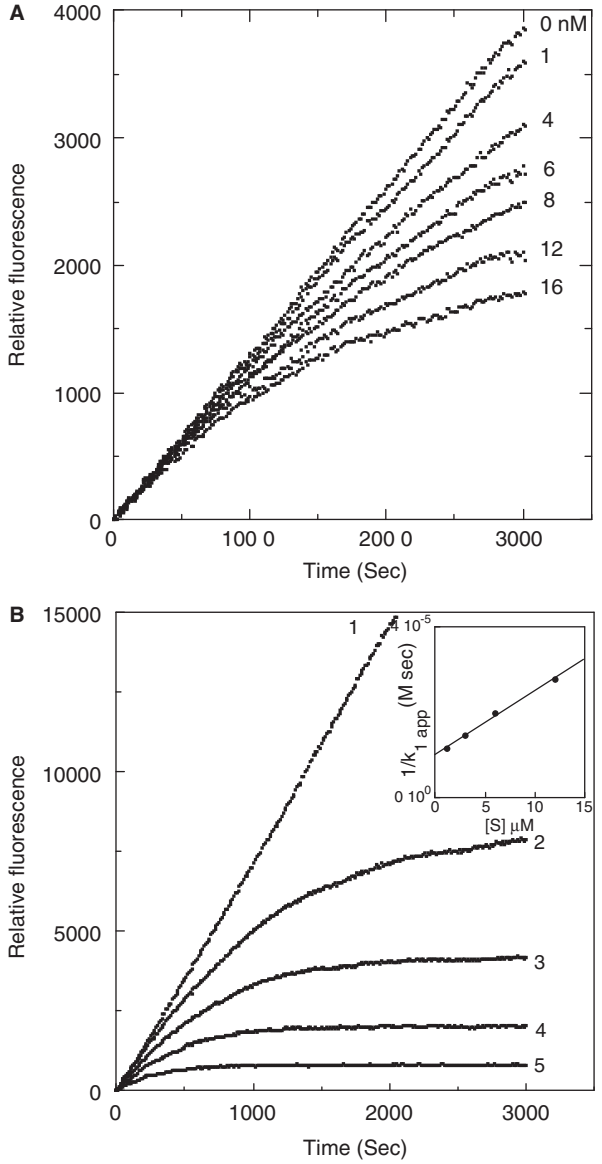

Fig. 8 Progress curves of fluorogenic substrate (Boc-EAR-MCA) hydrolysis by trypsin in the presence of BPTI. (A) Represents substrate (6 μM) hydrolysis by trypsin (1 nM) in the presence of varying concentrations of BPTI (0–16 nM). Inhibitor concentrations are shown on the right, adjacent to the respective curve. (B) Represents hydrolysis at varying concentrations of substrate (curves 1 and 2, 12 μM; 3, 6 μM; 4, 3 μM; 5, 1.2 μM) using trypsin (1 nM) and in the absence (curve 1) and in the presence (curves 2–5) of BPTI (16 nM). The apparent association rate constants ($k_{1\,app}$) for each substrate concentration are obtained from the respective curv es, using equation (*5*) (see 'Data analyses' section) and the value of k_1 was then obtained from a secondary plot of $1/k_{1\,app}$ versus [*S*], (inset).

in vivo, whereas mice with a genetic knockout of the gene for PN2/AβPP demonstrated a significant increase in thrombosis. Moreover, platelet PN2/AβPP transgenic mice developed larger haematomas in an experimental intracerebral haemorrhage model, whereas *AβPP* gene knockout mice exhibited reduced haemorrhage size. The question raised by these elegant studies relates to the mechanism by which overexpression of PN2/AβPP can inhibit thrombosis and enhance haemorrhage and deletion of this Kunitz inhibitor can promote thrombosis and inhibit haemorrhage. The present studies strongly suggest that the only plasma coagulation enzyme inhibited by physiological concentrations of PN2KPI achievable in plasma is FXIa. Thus, as shown in Table I, FXIa is inhibited by PN2KPI with a $K_i \sim 0.81$ nM, a concentration considerably higher than the virtually undetectable level of PN2/AβPP in plasma (*19*, *53*), but well below the concentrations (3–5 nM) that can be achieved at physiologic concentrations of platelets

after secretion from α-granules (*19*, *23*). Thus, in the vicinity of a platelet thrombus, the concentration of PN2/AβPP is likely to be sufficient to regulate FXIa activity, but insufficient to have any significant effect on other plasma serine proteases, K_i values (183–5500 nM) for which are 36-fold to 1,100-fold higher than the inhibitor concentration (3–5 nM) achieved after platelet secretion.

In reported specificity studies of target plasma proteases inhibited by PN2/AβPP and by PN2KPI, there is a general consensus that neither thrombin (*21*, *54*) nor FXIIa (*21*, *40*) is inhibited by PN2KPI, in agreement with the present studies which show no inhibition by thrombin and a $K_i \sim 7610$ nM for FXIIa (Table I). There is also a consensus that both FXIa (*18*, *21*, *40*, *55*) and trypsin (*18*, *21*, *40*) are potently inhibited by PN2KPI with K_i values of 0.25–2.7 nM and 0.02–0.42 nM, respectively, *i.e.* similar values to those reported herein (0.81 nM and 0.03 nM, respectively, Table I). In contrast, the highly homologous plasma protease, kallikrein is inhibited with a K_i (183 nM, Table I) >35-fold higher than the concentration of PN2/AβPP (3–5 nM) achieved after platelet secretion, compared with a value of 515 nM obtained by Dennis *et al.* (*55*) and no inhibition observed by Van Nostrand *et al.* (*21*), suggesting that kallikrein is not a target for inhibition by PN2/AβPP under physiological conditions. In contrast, widely divergent results have been reported for FIXa inhibition, as Schmaier *et al.* (*56*) have reported a K_i value of 190 nM for PN2KPI, and have shown that the presence of phospholipid (PS/PC) vesicles and FVIIIa protect FIXa from inhibition (*57*), whereas, in contrast, Neuenschwander *et al.* (*45*) have reported a K_i value of 9,500 nM for FIXa inhibition by PN2KPI, in reasonably good agreement with our K_i value of 5,500 nM (Table I). Similar discrepancies exist for inhibition of FXa by PN2KPI because Mahdi *et al.* (*58*) have reported K_i values of 33–72 nM, whereas Van Nostrand *et al.* (*21*) initially reported no inhibition and subsequently reported a K_i value of 59 nM (*40*), whereas Dennis *et al.* (*55*) reported a K_i value of 240 nM, compared with our value of 1,150 nM (Table I). Finally, Mahdi *et al.* (*59*) found that PN2KPI inhibited FVIIa with K_i values of 110–150 nM in the absence of tissue factor, compared with >1,000 nM reported by Dennis *et al.* (*55*) and 3,500 nM in the present study (Table I). In the presence of tissue factor, PN2KPI is a slightly more effective inhibitor of FVIIa, with K_i values of 68–78 nM reported by Schmaier *et al.* (*59*), compared with 300 nM reported by Dennis *et al.* (*55*) and 756 nM in the present study (Table I). The conclusion to be drawn from all these studies and the data presented herein is that, among all the plasma coagulation proteases examined for inhibition by PN2KPI, FXIa is the only physiologically relevant target, considering the concentrations of this Kunitz inhibitor achievable in the vicinity of a haemostatic thrombus.

In addition to determining the specificity PN2KPI for FXIa and trypsin the present work focuses on elucidating the mechanisms of inhibition of FXIa and trypsin, by the two structurally similar Kunitz-type inhibitors, PN2KPI and BPTI. The inhibition of FXIa by PN2KPI was studied in detail previously (*23*, *24*), and trypsin inhibition by BPTI has been characterized as a slow, tight-binding interaction (*44*). However, the precise mechanism of FXIa inhibition by either PN2KPI or BPTI and the mechanism of trypsin inhibition by PN2KPI are unknown. It is particularly interesting to determine these kinetic mechanisms and the functional roles of the P1 residues in these two inhibitors because of the high affinity and specificity of FXIa inhibition by PN2KPI, the marked difference in K_i for FXIa inhibition by PN2KPI and BPTI and the striking structural similarity between these two inhibitors in complex with their cognate proteases (Fig. 2). The present investigations demonstrate marked differences in equilibrium inhibition constants for FXIa inhibition by PN2KPI (K_i 0.81 nM) and BPTI (K_i 627 nM) as shown in Table III. Moreover, progress curve analyses demonstrated characteristic differences in the mechanisms of FXIa inhibition by PN2KPI and BPTI. Thus, the inhibition of FXIa by PN2KPI, by PN2KPI-R15 K, and by BPTI-K15 R were all demonstrated to conform to mechanism 1 (Fig. 1), in which a slow equilibration occurs between the enzyme and the inhibitor. In contrast, FXIa inhibition by BPTI conforms to a simple steady-sate kinetic mechanism (Fig. 5A), and analysis of the Michaelis–Menten plot (Fig. 5B) demonstrated competitive inhibitory mechanism, from which it can be calculated that the value of $K_{i\,cal}$ is 708 nM, which compares favourably with the value of $K_{i\,eq}$ (627 nM), determined from equilibrium inhibition experiments (Table III). Although there are reports on the inhibition of serine proteases by BPTI (*26*, *27*) this is the first report on the mechanism of FXIa inhibition by BPTI that is best described as classical competitive inhibition. These results are interesting in the context of recent studies by Neuenschwander *et al.* (*45*), who have demonstrated that the inhibition of FIXa by PN2KPI ($K_i \sim 20$ μM) proceeds by mechanism 2 (*45*), in contrast to our results for FXIa inhibition by PN2KPI (K_i 0.81 nM), which are consistent with mechanism 1.

The results of FXIa inhibition by the two Kunitz inhibitors stand in marked contrast to those describing trypsin inhibition by PN2KPI and BPTI. Thus, the equilibrium inhibition constants for trypsin inhibition by PN2KPI (K_i 0.026 nM) and BPTI (K_i 0.072 nM) are only ~3-fold different, compared with the ~775-fold difference when FXIa is the protease (Table III). Progress curve analyses demonstrate that the formation of the trypsin–PN2KPI complex and the trypsin–BPTI complex, like FXIa inhibition by PN2KPI, conform to mechanism 1. However, as mentioned in the 'Results' section, we were unable to obtain kinetic constants of trypsin inhibition by BPTI from these progress curves since reliable k_{obs} values could not be generated. Instead, the association rate constant (k_1) was obtained from separate sets of experiments designed to obtain kinetic parameters for irreversible kinetics (*44*). As shown in Fig. 8B, product formation [P_∞] approaches a constant value with time. Using this approach, we were able to obtain the association rate constant of trypsin inhibition by BPTI (Table III). These results do not exclude the possibility

of reversible enzyme–inhibitor binding with a dissociation rate too slow to be measured during the time interval studied. Indeed the value of the dissociation rate constant k_{-1} ($3.2 \times 10^{-5}\,s^{-1}$) shown in Table III for trypsin-BPTI complex was found to be 10-fold slower ($3.2 \times 10^{-4}\,s^{-1}$) than that of FXIa-PN2KPI (Table III).

In addition to establishing the mechanistic characteristics describing the two Kunitz inhibitors, PN2KPI and BPTI, in FXIa and trypsin inhibition, we further investigated the importance of P1 site residues, *i.e.* Arg^{15} in PN2KPI and Lys^{15} in BPTI, in FXIa inhibition. The essential role of the P1 residue of PN2KPI was previously demonstrated in our laboratory by using a mutant protein, PN2KPI-R15A, which completely loses its inhibitory activity against FXIa (*28*). In addition, it has been demonstrated that the BPTI (K15A) mutant largely lost its trypsin inhibitory activity (*60*). As shown in Fig. 2, loop 1 of the enzyme-interacting double-loop region contains the P1 residue and is stabilized by a disulfide bond. This loop structure maintains similar backbone orientations in several Kunitz inhibitors, including PN2KPI and BPTI (Fig. 2B). The P1 residue of inhibitors in general is considered to be the most energetically important residue for high-affinity binding to serine proteases and therefore the primary determinant of specificity of an inhibitor for a given protease (*61*, *62*). The guanidinium group of Arg^{15} in PN2KPI interacts directly with the carboxylate group of Asp^{189} in trypsin (PDB: 1TAW) (*41*) and of Asp^{189} in the catalytic domain of FXIa (PDB:1ZJD) (*28*) by forming a salt bridge in the S1 specificity pocket (Fig. 2C). Similarly, Lys^{15} in BPTI protrudes into the S1 specificity pocket of trypsin, while maintaining the same side chain orientation (similar to Arg^{15}) and interacts with Asp^{189}. However, the shorter Lys side chain (compared to Arg) relies on an ordered water molecule to establish the Lys^{15}-Asp^{189} interaction in the BPTI–trypsin complex (Fig. 2D), (PDB:2FTL) (*29*). Thus, whereas PN2KPI and BPTI have similar backbone structures and P1 residue side chain orientations, differences in side chain bulkiness, length and consequent charge distribution, result in significant differences in local intermolecular interactions with FXIa. We hypothesized that these fine structural differences between PN2KPI and BPTI might have functional consequences.

To determine whether the presence of Arg^{15} or Lys^{15} at the P1 site of the inhibitor interacting with Asp^{189} of the protease translates into functional differences in their capacity to inhibit FXIa, P1 site PN2KPI and BPTI swap mutants along with their native parent molecules were examined for their inhibitory properties. Unlike the complete or near complete loss of enzyme inhibitory activity observed with alanine mutants of these inhibitors (*28*, *60*), the mutant, PN2KPI-R15 K displayed partial loss of function, as previously observed (*40*). BPTI-K15 R on the other hand displayed >150-fold gain of function (K_i 4.1 nM) in FXIa inhibition, compared to its native counterpart BPTI (K_i 627 nM). The inhibitory activities for FXIa of the Arg^{15}-containing PN2KPI and the BPTI-K15 R mutant are ~14-fold and ~150-fold more potent than those of the corresponding Lys^{15}-containing forms. Thus, Arg^{15} is an important determinant of high-affinity binding and specificity for FXIa inhibition. In contrast, the presence of arginine or lysine at the P1 position had very little influence on the trypsin inhibitory activities of either PN2KPI or BPTI. Thus, the presence of arginine at the P1 position in BPTI or PN2KPI only slightly improves (5-fold and 2-fold, respectively) their affinity for trypsin. In an earlier study of the crystal structure of uncomplexed trypsin-D189 S (PDB: 1AMH) a single amino acid mutation in the substrate-binding pocket resulted in extensive structural changes around the mutated residue (*63*). However, a structural comparison of native trypsin with that of BPTI complexed to trypsin-D189 S revealed striking structural similarities (*64*), indicating the plasticity of trypsin accommodating BPTI and reverting back to its native structure. Thus, the structural plasticity of trypsin may explain why similar inhibition constants are seen with arginine or lysine containing Kunitz inhibitors. In contrast, in the case of FXIa the presence of Arg or Lys at the P1 site of the inhibitor determines both proteinase specificity and the kinetic mechanisms of proteinase interaction. The results of our mutational analysis of key residues in PN2KPI, based on the crystal structures of PN2KPI and BPTI in complex with their cognate proteinases (Table II) are particularly relevant in the context of the additional studies summarized in Table III, suggesting that it is the plasticity of trypsin that renders it particularly susceptible to inhibition by Kunitz inhibitors. Thus, it would appear that PN2/AβPP, contained within the α-granules of platelets and secreted into the vicinity of the haemostatic thrombus, is an exquisitely specific inhibitor of FXIa among all other plasma coagulation proteases since, within the vascular compartment, it would not encounter trypsin, a digestive enzyme secreted into the gastrointestinal tract.

Supplementary Data

Supplementary Data are available at *JB* online.

Acknowledgements

We are grateful to Sriram Krishnaswamy (Children's Hospital of the University of Pennsylvania), Paul Bock (Vanderbilt University School of Medicine) and Barrie Ashby (Temple University School of Medicine) for helpful discussions concerning the design and kinetic analysis of data. We thank Patricia Pileggi for help in manuscript preparation.

Funding

Supported by research grants from the National Institutes of Health (HL74124 and HL46213 to P.N.W.).

Conflict of interest

No conflict of interest.

References

1. Page, M.J. and Di Cera, E. (2008) Serine peptidases: classification, structure and function. *Cell. Mol. Life Sci.* **65**, 1220–1236
2. Walsh, P.N. (2001) Factor XI, in *Hemostasis and Thrombosis: Basic Principles & Clinical Practice*

(Colman, R.W., Hirsh, J., Marder, V.J., Clowes, A.W., and George, J.N., eds.), pp. 191–202, Lippincott Williams & Wilkins, Philadelphia
3. Bouma, B.N. and Griffin, J.H. (1977) Human blood coagulation factor XI. Purification, properties, and mechanism of activation by activated factor XII. *J. Biol. Chem.* **252**, 6432–6437
4. Naito, K. and Fujikawa, K. (1991) Activation of human blood coagulation factor XI independent of factor XII. Factor XI is activated by thrombin and factor XIa in the presence of negatively charged surfaces. *J. Biol. Chem.* **266**, 7353–7358
5. Gailani, D. and Broze, G.J. Jr (1991) Factor XI activation in a revised model of blood coagulation. *Science* **253**, 909–912
6. Walsh, P.N. and Griffin, J.H. (1981) Contributions of human platelets to the proteolytic activation of blood coagulation factors XII and XI. *Blood* **57**, 106–118
7. Fujikawa, K., Legaz, M.E., Kato, H., and Davie, E.W. (1974) The mechanism of activation of bovine factor IX (Christmas factor) by bovine factor XIa (activated plasma thromboplastin antecedent). *Biochemistry* **13**, 4508–4516
8. Di Scipio, R.G., Kurachi, K., and Davie, E.W. (1978) Activation of human factor IX (Christmas factor). *J. Clin. Invest.* **61**, 1528–1538
9. Osterud, B., Bouma, B.N., and Griffin, J.H. (1978) Human blood coagulation factor IX. Purification, properties, and mechanism of activation by activated factor XI. *J. Biol. Chem.* **253**, 5946–5951
10. Sinha, D., Seaman, F.S., and Walsh, P.N. (1987) Role of calcium ions and the heavy chain of factor XIa in the activation of human coagulation factor IX. *Biochemistry* **26**, 3768–3775
11. Knauer, D.J., Majumdar, D., Fong, P.C., and Knauer, M.F. (2000) SERPIN regulation of factor XIa. The novel observation that protease nexin 1 in the presence of heparin is a more potent inhibitor of factor XIa than C1 inhibitor. *J. Biol. Chem.* **275**, 37340–37346
12. Damus, P.S., Hicks, M., and Rosenberg, R.D. (1973) Anticoagulant action of heparin. *Nature* **246**, 355–357
13. Wuillemin, W.A., Eldering, E., Citarella, F., de Ruig, C.P., ten Cate, H., and Hack, C.E. (1996) Modulation of contact system proteases by glycosaminoglycans. Selective enhancement of the inhibition of factor XIa. *J. Biol. Chem.* **271**, 12913–12918
14. Forbes, C.D., Pensky, J., and Ratnoff, O.D. (1970) Inhibition of activated Hageman factor and activated plasma thromboplastin antecedent by purified serum C1 inactivator. *J. Lab. Clin. Med.* **76**, 809–815
15. Scott, C.F., Schapira, M., James, H.L., Cohen, A.B., and Colman, R.W. (1982) Inactivation of factor XIa by plasma protease inhibitors: predominant role of alpha 1-protease inhibitor and protective effect of high molecular weight kininogen. *J. Clin. Invest.* **69**, 844–852
16. Heck, L.W. and Kaplan, A.P. (1974) Substrates of Hageman factor. I. Isolation and characterization of human factor XI (PTA) and inhibition of the activated enzyme by alpha 1-antitrypsin. *J. Exp. Med.* **140**, 1615–1630
17. Saito, H., Goldsmith, G.H., Moroi, M., and Aoki, N. (1979) Inhibitory spectrum of alpha 2-plasmin inhibitor. *Proc. Natl Acad. Sci. USA* **76**, 2013–2017
18. Smith, R.P., Higuchi, D.A., and Broze, G.J. Jr (1990) Platelet coagulation factor XIa-inhibitor, a form of Alzheimer amyloid precursor protein. *Science* **248**, 1126–1128
19. Van Nostrand, W.E., Schmaier, A.H., Farrow, J.S., and Cunningham, D.D. (1990) Protease nexin-II (amyloid beta-protein precursor): a platelet alpha-granule protein. *Science* **248**, 745–748
20. Bush, A.I., Martins, R.N., Rumble, B., Moir, R., Fuller, S., Milward, E., Currie, J., Ames, D., Weidemann, A., Fischer, P., Multhaup, G., Beyreuther, K., and Masters, C.L. (1990) The amyloid precursor protein of Alzheimer's disease is released by human platelets. *J. Biol. Chem.* **265**, 15977–15983
21. Van Nostrand, W.E., Wagner, S.L., Farrow, J.S., and Cunningham, D.D. (1990) Immunopurification and protease inhibitory properties of protease nexin- 2/amyloid beta-protein precursor. *J. Biol. Chem.* **265**, 9591–9594
22. Zhang, Y., Scandura, J.M., Van Nostrand, W.E., and Walsh, P.N. (1997) The mechanism by which heparin promotes the inhibition of coagulation factor XIa by protease nexin-2. *J. Biol. Chem.* **272**, 26139–26144
23. Scandura, J.M., Zhang, Y., Van Nostrand, W.E., and Walsh, P.N. (1997) Progress curve analysis of the kinetics with which blood coagulation factor XIa is inhibited by protease nexin-2. *Biochemistry* **36**, 412–420
24. Badellino, K.O. and Walsh, P.N. (2000) Protease nexin II interactions with coagulation factor XIa are contained within the Kunitz protease inhibitor domain of protease nexin II and the factor XIa catalytic domain. *Biochemistry* **39**, 4769–4777
25. Badellino, K.O. and Walsh, P.N. (2001) Localization of a heparin binding site in the catalytic domain of factor XIa. *Biochemistry* **40**, 7569–7580
26. Grzesiak, A., Krokoszynska, I., Krowarsch, D., Buczek, O., Dadlez, M., and Otlewski, J. (2000) Inhibition of six serine proteinases of the human coagulation system by mutants of bovine pancreatic trypsin inhibitor. *J. Biol. Chem.* **275**, 33346–33352
27. Stassen, J.M., Lambeir, A.M., Matthyssens, G., Ripka, W.C., Nystrom, A., Sixma, J.J., and Vermylen, J. (1995) Characterisation of a novel series of aprotinin-derived anticoagulants. I. In vitro and pharmacological properties. *Thromb. Haemost.* **74**, 646–654
28. Navaneetham, D., Jin, L., Pandey, P., Strickler, J.E., Babine, R.E., Abdel-Meguid, S.S., and Walsh, P.N. (2005) Structural and mutational analyses of the molecular interactions between the catalytic domain of factor XIa and the Kunitz protease inhibitor domain of protease nexin 2. *J. Biol. Chem.* **280**, 36165–36175
29. Hanson, W.M., Domek, G.J., Horvath, M.P., and Goldenberg, D.P. (2007) Rigidification of a flexible protease inhibitor variant upon binding to trypsin. *J. Mol. Biol.* **366**, 230–243
30. McEvoy, M.D., Reeves, S.T., Reves, J.G., and Spinale, F.G. (2007) Aprotinin in cardiac surgery: a review of conventional and novel mechanisms of action. *Anesth. Analg.* **105**, 949–962
31. Henry, D., Carless, P., Fergusson, D., and Laupacis, A. (2009) The safety of aprotinin and lysine-derived antifibrinolytic drugs in cardiac surgery: a meta-analysis. *CMAJ* **180**, 183–193
32. Scott, C.F., Wenzel, H.R., Tschesche, H.R., and Colman, R.W. (1987) Kinetics of inhibition of human plasma kallikrein by a site-specific modified inhibitor Arg15-aprotinin: evaluation using a microplate system and comparison with other proteases. *Blood* **69**, 1431–1436
33. Salameh, M.A., Soares, A.S., Hockla, A., and Radisky, E.S. (2008) Structural basis for accelerated cleavage of bovine pancreatic trypsin inhibitor (BPTI) by human mesotrypsin. *J. Biol. Chem.* **283**, 4115–4123

34. Waxman, L., Smith, D.E., Arcuri, K.E., and Vlasuk, G.P. (1990) Tick anticoagulant peptide (TAP) is a novel inhibitor of blood coagulation factor Xa. *Science* **248**, 593–596
35. Krishnaswamy, S., Vlasuk, G.P., and Bergum, P.W. (1994) Assembly of the prothrombinase complex enhances the inhibition of bovine factor Xa by tick anticoagulant peptide. *Biochemistry* **33**, 7897–7907
36. Rezaie, A.R. (2004) Kinetics of factor Xa inhibition by recombinant tick anticoagulant peptide: both active site and exosite interactions are required for a slow- and tight-binding inhibition mechanism. *Biochemistry* **43**, 3368–3375
37. Macedo-Ribeiro, S., Almeida, C., Calisto, B.M., Friedrich, T., Mentele, R., Sturzebecher, J., Fuentes-Prior, P., and Pereira, P.J. (2008) Isolation, cloning and structural characterisation of boophilin, a multifunctional Kunitz-type proteinase inhibitor from the cattle tick. *PLoS ONE* **3**, e1624
38. Petersen, L.C., Bjorn, S.E., Olsen, O.H., Nordfang, O., Norris, F., and Norris, K. (1996) Inhibitory properties of separate recombinant Kunitz-type-protease-inhibitor domains from tissue-factor-pathway inhibitor. *Eur. J. Biochem.* **235**, 310–316
39. Sierko, E., Wojtukiewicz, M.Z., and Kisiel, W. (2007) The role of tissue factor pathway inhibitor-2 in cancer biology. *Semin. Thromb. Hemost.* **33**, 653–659
40. Van Nostrand, W.E., Schmaier, A.H., Siegel, R.S., Wagner, S.L., and Raschke, W.C. (1995) Enhanced plasmin inhibition by a reactive center lysine mutant of the Kunitz-type protease inhibitor domain of the amyloid beta-protein precursor. *J. Biol. Chem.* **270**, 22827–22830
41. Scheidig, A.J., Hynes, T.R., Pelletier, L.A., Wells, J.A., and Kossiakoff, A.A. (1997) Crystal structures of bovine chymotrypsin and trypsin complexed to the inhibitor domain of Alzheimer's amyloid beta-protein precursor (APPI) and basic pancreatic trypsin inhibitor (BPTI): engineering of inhibitors with altered specificities. *Protein Sci.* **6**, 1806–1824
42. Perona, J.J., Tsu, C.A., Craik, C.S., and Fletterick, R.J. (1993) Crystal structures of rat anionic trypsin complexed with the protein inhibitors APPI and BPTI. *J. Mol. Biol.* **230**, 919–933
43. Hynes, T.R., Randal, M., Kennedy, L.A., Eigenbrot, C., and Kossiakoff, A.A. (1990) X-ray crystal structure of the protease inhibitor domain of Alzheimer's amyloid beta-protein precursor. *Biochemistry* **29**, 10018–10022
44. Zhou, J.M., Liu, C., and Tsou, C.L. (1989) Kinetics of trypsin inhibition by its specific inhibitors. *Biochemistry* **28**, 1070–1076
45. Neuenschwander, P.F., Williamson, S.R., Nalian, A., and Baker-Deadmond, K.J. (2006) Heparin modulates the 99-loop of factor IXa: effects on reactivity with isolated Kunitz-type inhibitor domains. *J. Biol. Chem.* **281**, 23066–23074
46. Cha, S. (1975) Tight-binding inhibitors-I. Kinetic behavior. *Biochem. Pharmacol.* **24**, 2177–2185
47. Morrison, J.F. (1982) The slow-binding and slow, tight-binding inhibition of enzyme-catalysed reactions. *Trends Biochem. Sci.* **7**, 102–105
48. Morrison, J.F. and Walsh, C.T. (1988) The behavior and significance of slow-binding enzyme inhibitors. *Adv. Enzymol. Relat. Areas Mol. Biol.* **61**, 201–301
49. Huang, Z.F., Wun, T.C., and Broze, G.J. Jr (1993) Kinetics of factor Xa inhibition by tissue factor pathway inhibitor. *J. Biol. Chem.* **268**, 26950–26955
50. Vincent, J.P. and Lazdunski, M. (1972) Trypsin-pancreatic trypsin inhibitor association. Dynamics of the interaction and role of disulfide bridges. *Biochemistry* **11**, 2967–2977
51. Baird, T.R. and Walsh, P.N. (2002) The interaction of factor XIa with activated platelets but not endothelial cells promotes the activation of factor IX in the consolidation phase of blood coagulation. *J. Biol. Chem.* **277**, 38462–38467
52. Xu, F., Davis, J., Miao, J., Previti, M.L., Romanov, G., Ziegler, K., and Van Nostrand, W.E. (2005) Protease nexin-2/amyloid beta-protein precursor limits cerebral thrombosis. *Proc. Natl. Acad. Sci. USA* **102**, 18135–18140
53. Komiyama, Y., Murakami, T., Egawa, H., Okubo, S., Yasunaga, K., and Murata, K. (1992) Purification of factor XIa inhibitor from human platelets. *Thromb. Res.* **66**, 397–408
54. Sinha, S., Dovey, H.F., Seubert, P., Ward, P.J., Blacher, R.W., Blaber, M., Bradshaw, R.A., Arici, M., Mobley, W.C., and Lieberburg, I. (1990) The protease inhibitory properties of the Alzheimer's beta-amyloid precursor protein. *J. Biol. Chem.* **265**, 8983–8985
55. Dennis, M.S. and Lazarus, R.A. (1994) Kunitz domain inhibitors of tissue factor-factor VIIa. II. Potent and specific inhibitors by competitive phage selection. *J. Biol. Chem.* **269**, 22137–22144
56. Schmaier, A.H., Dahl, L.D., Rozemuller, A.J., Roos, R.A., Wagner, S.L., Chung, R., and Van Nostrand, W.E. (1993) Protease nexin-2/amyloid beta protein precursor. A tight-binding inhibitor of coagulation factor IXa. *J. Clin. Invest.* **92**, 2540–2545
57. Schmaier, A.H., Dahl, L.D., Hasan, A.A., Cines, D.B., Bauer, K.A., and Van Nostrand, W.E. (1995) Factor IXa inhibition by protease nexin-2/amyloid beta-protein precursor on phospholipid vesicles and cell membranes. *Biochemistry* **34**, 1171–1178
58. Mahdi, F., Van Nostrand, W.E., and Schmaier, A.H. (1995) Protease nexin-2/amyloid beta-protein precursor inhibits factor Xa in the prothrombinase complex. *J. Biol. Chem.* **270**, 23468–23474
59. Mahdi, F., Rehemtulla, A., Van Nostrand, W.E., Bajaj, S.P., and Schmaier, A.H. (2000) Protease nexin-2/Amyloid beta-protein precursor regulates factor VIIa and the factor VIIa-tissue factor complex. *Thromb. Res.* **99**, 267–276
60. Castro, M.J. and Anderson, S. (1996) Alanine point-mutations in the reactive region of bovine pancreatic trypsin inhibitor: effects on the kinetics and thermodynamics of binding to beta-trypsin and alpha-chymotrypsin. *Biochemistry* **35**, 11435–11446
61. Bode, W. and Huber, R. (1992) Natural protein proteinase inhibitors and their interaction with proteinases. *Eur. J. Biochem.* **204**, 433–451
62. Laskowski, M. Jr and Kato, I. (1980) Protein inhibitors of proteinases. *Annu. Rev. Biochem.* **49**, 593–626
63. Szabo, E., Bocskei, Z., Naray-Szabo, G., and Graf, L. (1999) The three-dimensional structure of Asp189Ser trypsin provides evidence for an inherent structural plasticity of the protease. *Eur. J. Biochem.* **263**, 20–26
64. Perona, J.J., Hedstrom, L., Wagner, R.L., Rutter, W.J., Craik, C.S., and Fletterick, R.J. (1994) Exogenous acetate reconstitutes the enzymatic activity of trypsin Asp189Ser. *Biochemistry* **33**, 3252–3259